Medlin, J. M., G. T. Stano, and B. F. Daly, 2012: Diagnosis of a dense fog event using MODIS and high resolution GOES satellite products with direct model output. *Electronic J. Operational Meteor.*, **13** (2), 15–31.

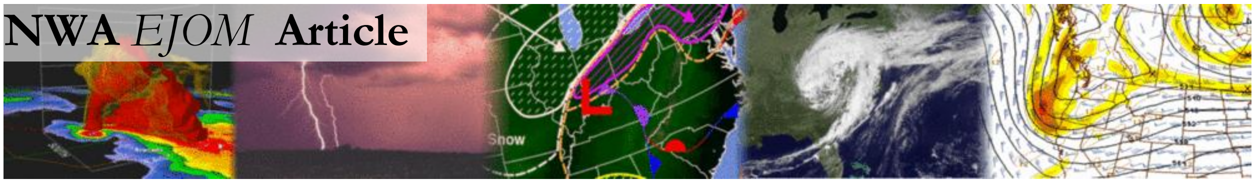

Diagnosis of a Dense Fog Event using MODIS and High Resolution GOES Satellite Products with Direct Model Output

JEFFREY M. MEDLIN
National Weather Service, Mobile, Alabama

GEOFFREY T. STANO
NASA SPoRT/ENSCO, Inc., Huntsville, Alabama

BRIAN F. DALY
National Weather Service, Mobile, Alabama

(Manuscript received 24 October 2011; in final form 20 February 2012)

ABSTRACT

This paper presents an analysis of an evolving dense fog event that occurred within the United States Central Gulf Coast Region during the early morning hours of 17 February 2011. Seasonal climatology, pre-event synoptic conditions and a thorough diagnosis of ongoing processes in the hours leading up to the event all suggested dense fog formation was likely. Mesoscale model forecasts of outgoing longwave radiation between 200-300 W m^{-2} and eventual sensible cloud heights <150 m yielded initial clues as to when the dense fog may form and how it may be distributed. Subsequent passes of the Moderate Resolution Imaging Spectroradiometer and the Geostationary Operational Environmental Satellite provided high spatial and temporal resolution observational confirmation regarding the development, timing and location of the fog and an ability to adjust the forecast based on the latest available fog product. Although polar orbiting satellite data are received relatively infrequently, it is shown how utilizing these during an evolving fog situation may either grant or dissuade a forecaster's confidence regarding the outcome.

1. Introduction and background

Dense fog (visibility <0.4 km) developed over southwestern Alabama and the extreme western Florida Panhandle region during the early morning hours of 17 February 2011. Figure 1 is one of the first discernible Geostationary Operational Environmental Satellite (GOES) images valid 1331 UTC and markedly verifies the horizontal extent of the fog which formed between ~0500-1000 UTC. The greatest average number of dense fog days occurs near the coastline and

Corresponding author address: Jeffrey Medlin, National Weather Service, 8400 Airport Blvd., Bldg. 11, Mobile, AL 36608. E-mail: jeffrey.medlin@noaa.gov

during the early morning hours of the cool season (Dec-May) within this U.S. region (Croft et al., 1995; Croft et al., 1997). It is also worth noting that this U.S. region has experienced several relatively recent high impact dense fog events with far reaching local impacts (e.g., the 1992 Amtrak Train Derailment disaster occurring over the Mobile River Delta and the 1995 Great Mobile Bayway Dense Fog Disaster; Medlin and Croft 1996).

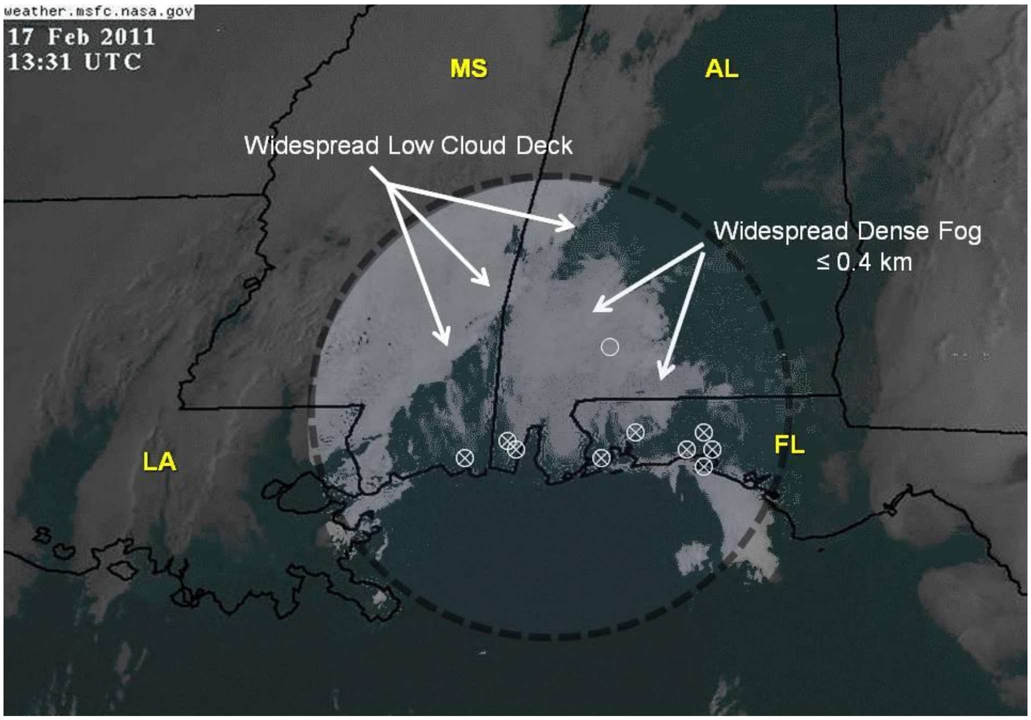

Figure 1. GOES visible image valid 1331 UTC 17 February 2011. The region of concern is over southwestern Alabama and the extreme western Florida Panhandle. White station circles with an "X" in the middle represent a total obscuration of vertical visibility while open circles represent a partial obscuration. All stations reported horizontal surface visibilities ≤0.4 km (or ≤0.25 SM) around 1250 UTC. The region within the spyglass was enhanced to show the gradient of fog along the Alabama and western Florida coastal zone.

While this study examines the synoptic and mesoscale evolutionary details of the event, its purpose is to also show how Moderate Resolution Imaging Spectroradiometer (MODIS) satellite imagery (Barnes et al., 1998; Guenther et al., 1998) can be integrated into the forecast process to assist with critical forecast decision making. The MODIS products used in this study are the sea surface temperatures (SSTs) and the fog product. These are provided in real time to several National Weather Service (NWS) forecast offices through a partnership with the National Aeronautics and Space Administration's (NASA) Short-term Prediction Research and Transition (SPoRT) program located in Huntsville, Alabama and are available on the Advanced Weather Interactive Processing System (AWIPS) Platform. Section 2 of this paper describes data used and corresponding product descriptions. Section 3 of this paper provides an assessment of the existing synoptic conditions prior to dense fog development. The analysis and discussion within Section 4 simulates the receipt of various data sources by a forecaster, discusses interpretations and how these may bolster or dissuade forecast confidence at various points in time leading up to the event outcome. Section 5 presents concluding thoughts associated with this event.

2. Data and product description

The MODIS SST composite, in collaboration with the Jet Propulsion Laboratory (Jedlovec et al. 2009), uses a combination of infrared MODIS data, microwave observations from the Advanced Microwave Scanning Radiometer–Earth Observing system (AMSR-E). They are produced over a given region four times daily corresponding to Terra and Aqua satellite equator crossing times (i.e., Terra day, Aqua day, Terra night, and Aqua night). For a given day and region, data from the previous fourteen days of MODIS and AMSR-E observations are used in the compositing. The MODIS data are only available in cloud free regions. The lower resolution AMSR-E microwave observations help reduce latency due to cloud cover. The AMSR-E instrument utilizes 12 channels and six frequencies from 6.9 to 89.0 GHz. The horizontally and vertically polarized radiation is measured separately for each frequency. More information can be found on the AMSR-E information page maintained by Marshall Space Flight Center (weather.msfc.nasa.gov/AMSR/instrument_descrip.html). For the SPoRT SST composite, SPoRT specifically used the 10.7 GHz frequency for SSTs at a 38 km resolution (Wentz and Meissner 2004). The AMSR-E microwave data is a tradeoff between the decreased spatial resolution of the AMSR-E data (25 km) and the increased coverage due to the near all weather capability. In this way the spatial structure observed in the 1km MODIS data is preserved and greatly reduces latency in the final product. The MODIS and AMSR-E data are then used at each 1 km pixel to form a weighted average based on their latency (number of days from the current day) and quality. Recent SST data are given more weight than older data. Furthermore, each dataset is individually weighted. The AMSR-E is given a weight of 20% compared to MODIS data.

The SPoRT SST composite described above uses both MODIS and AMSR-E retrievals of sea surface temperature. However, on 1 October 2011 the AMSR-E instrument failed and its contributions were no longer available (a replacement, AMSR2, will be launched by Japan, but this will not occur for at least a year). The AMSR-E observations were given a low weighting and were mainly used to reduce latency in the SPoRT SST composite to fill in data when MODIS data were unavailable. As a result, the loss of AMSR-E does not have a major impact on the SPoRT SST composite. SPoRT has since incorporated the daily NESDIS GOES-POES SST composite to fill in the missing data that AMSR-E used to provide. The NESDIS-GP is the GOES-POES sea surface temperature composite produced by STAR (Center for Satellite Applications and Research) within NESDIS (Maturi et al. 2010; STAR webpage). This scheme combines multi-satellite retrievals of sea surface datasets from polar and geostationary sources into a single global analysis. This analysis provides a daily, gap free map of the sea surface temperature at 0.1° resolution (STAR web page). The SPoRT SST composite has not been adversely affected and still produces a high resolution SST composite relying on the high resolution MODIS data. Ultimately, as this is not a climate product, SPoRT will continue to evolve the MODIS SST product to incorporate future, high-resolution data, such as from the Visible Infrared Imaging Radiometer Suite (VIIRS) and the follow-up to AMSR-E, AMSR2.

The second MODIS product used in the evaluation is the spectral difference product, commonly referred to as the fog product. The concept originates from the bi-spectral nighttime fog detection product described by Eyre et al. (1984) who used the Advanced Very High

Resolution Radiometer (AVHRR – Hastings and Emery 1992). This product takes advantage of the lower thermal emissivity of water clouds (3.9 µm) versus land surfaces (11 µm). A single subjectively determined threshold value (2.5 K) defines the cutoff region for fog/stratus versus clear skies in the image. The MODIS or GOES fog product displays the difference of the 11 µm minus the 3.9 µm channels. Water clouds have a lower thermal emissivity than land surfaces, while ice or mixed phase clouds would be equal to or greater than the land surface emissivity. Therefore, when fog or low stratus occurs the temperature difference, in Kelvin, will be positive. Locations with values greater than the threshold are labeled as fog. Conversely, regions with values lower than the threshold are clear. In reality, the threshold is not constant and can change spatially, temporally (time of night), and seasonally.

3. Pre-event synoptic conditions

On the afternoon prior to the dense fog event, the extension of a surface anticyclone was influencing the eastern Gulf of Mexico. The 1800 UTC 16 February surface analysis (Fig. 2) represents a time when the local atmosphere was mechanically well-mixed just before the near-surface radiation inversion began to form. Furthermore, it was verified by the 0000 UTC 17 February upper air analysis (not shown) that neither momentum transfer from aloft into the boundary layer nor advection of moisture into the mid- and/or high tropospheric levels would likely interfere with fog formation.

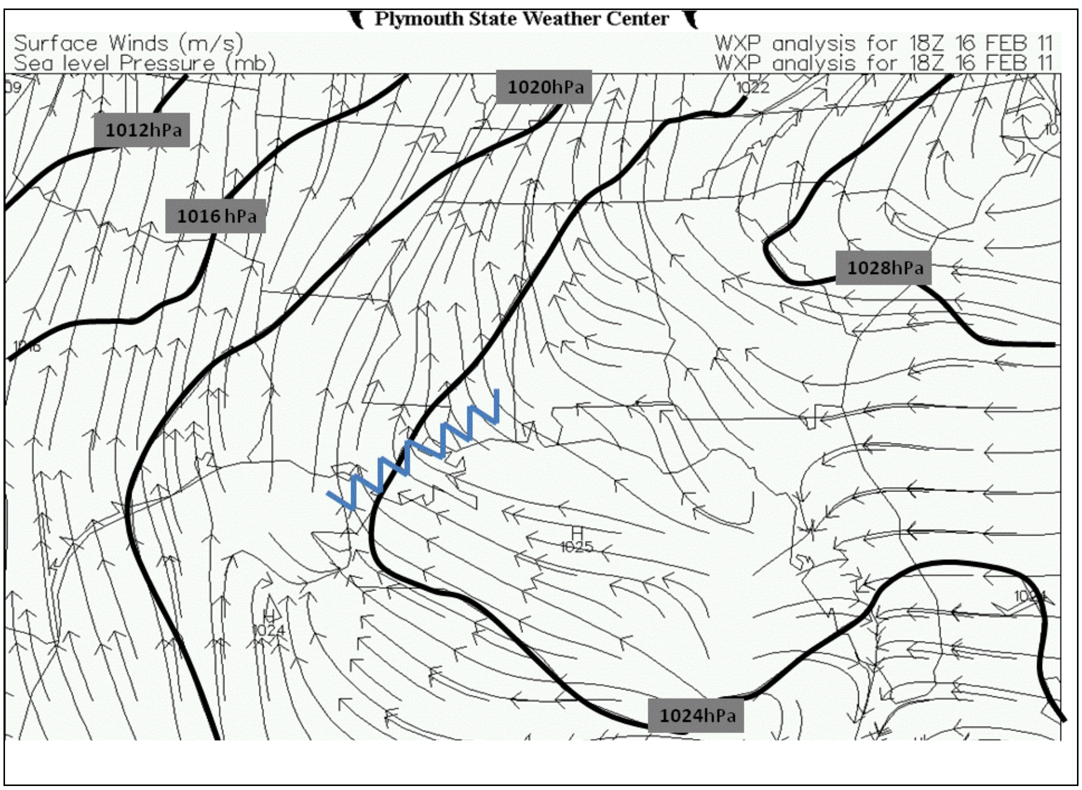

Figure 2. Mean sea level analysis (hPa) and surface streamlines valid 1800 UTC 16 February 2011 (courtesy Plymouth State University). Note westward extension of departing anticyclone and axis of anticyclonic curvature associated (blue zig-zag) forcing surface divergence along the U.S. Central Gulf Coast region (not shown).

The departing surface anticyclone in Figure 2 exhibited sharp anticyclonic curvature with observed regional boundary layer winds of ~5 m s^{-1} (10 kt) during the preceding daylight period. The diffluent streamlines were associated with computed surface divergence (not shown). This wind flow pattern provided ample opportunity for an upward flux of water vapor to be injected into the upstream flow. While the data suggest that moist static energy would increase as the overlying air passed over the warm water offshore, an ensuing cooling effect would occur as the air advected over the relatively cooler nearshore waters. The MODIS SST composite (Fig. 3) shows a strong thermal gradient over the near shore waters as temperatures quickly decrease from ~18 to 14 °C (or ~64 to 58 °F). The aforementioned cooling effect would allow the air, dewpoint, and sea surface temperatures to converge resulting in a subsequent additional local rise in stability.

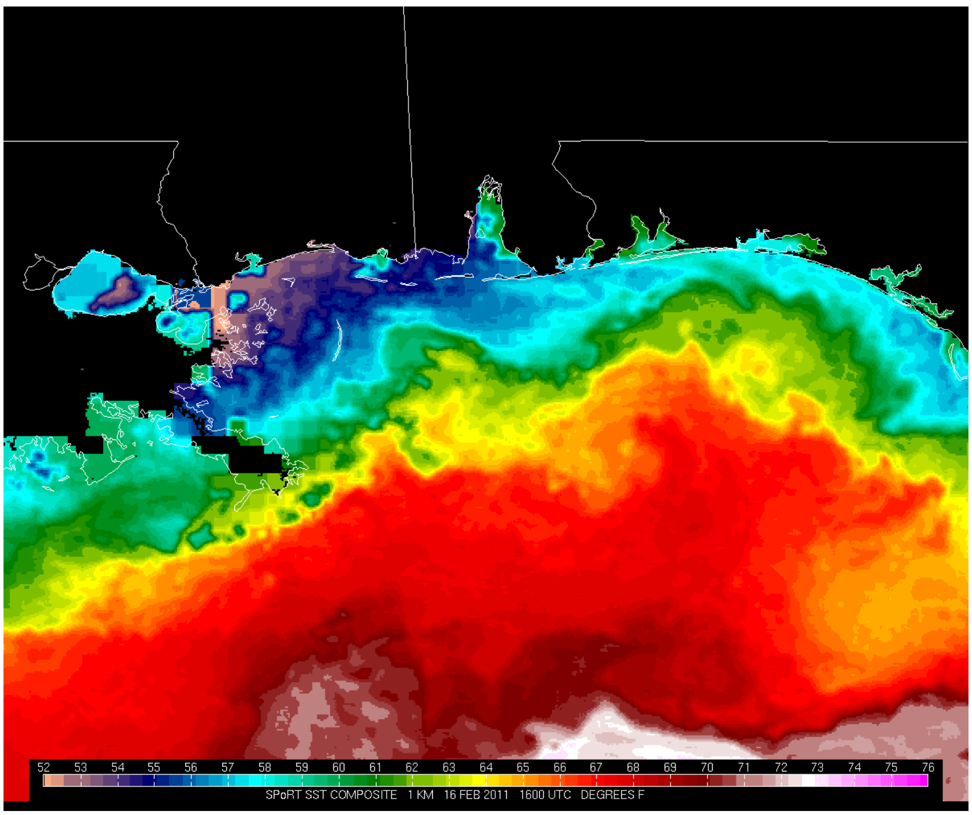

Figure 3. MODIS Sea Surface Temperature analysis (°F) valid at 1600 UTC 16 February 2011. Note the relatively cooler nearshore waters south of coastal Alabama and the extreme northwestern Florida Panhandle.

Figure 4 is a regional surface dew point depression analysis valid 0000 UTC 17 February. Of note is the great contrast between near saturated surface conditions just offshore to very dry air over interior southwest Alabama (upper 30s °F and dewpoint depressions >15 °F). This presents difficulty deciding just how far inland fog will develop, and if so, whether it would be dense? The 0000 UTC Slidell, LA (KLIX) sounding is shown in (Fig. 5). Within the surface-850 hPa layer, wind speeds were observed near ~7.5 m s^{-1} (15 kt) from the southeast, and dewpoint depressions averaged less than 1 °C. One may glean from Figures 4 and 5 that the area of near saturated air offshore was poised to advect inland and beneath a deep window of outgoing longwave radiation.

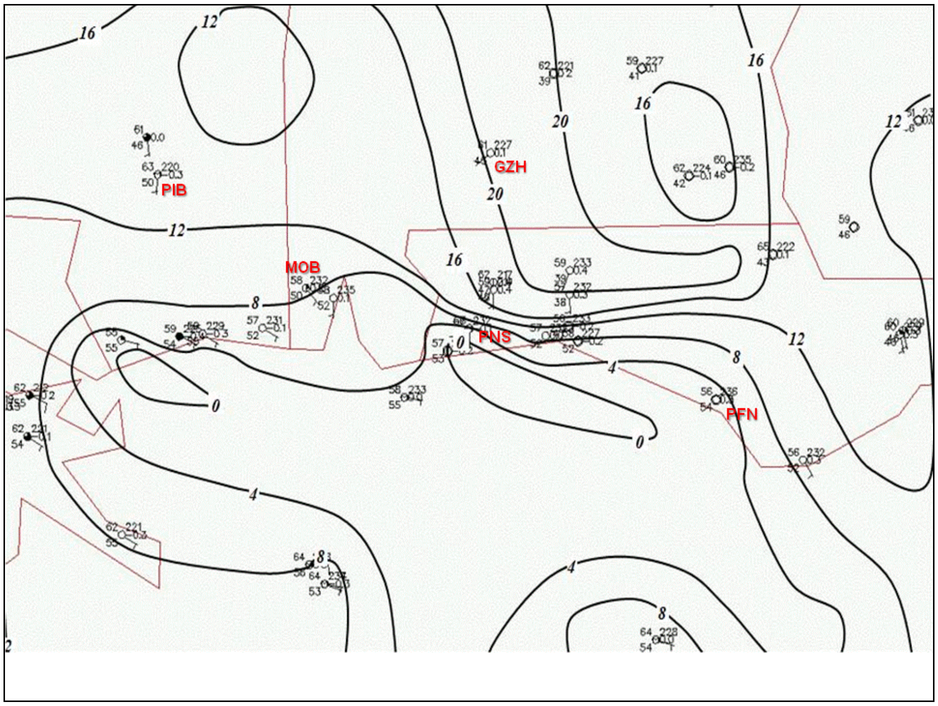

Figure 4. Local surface observations (courtesy Plymouth State University) with dewpoint depression analysis (°F) overlaid for 0000 UTC 17 February 2011. Contours are every 4 °F. Select METAR locations represent Mobile, AL (MOB), Pine Belt, MS (PIB), Evergreen, AL (GZH), Pensacola, FL (PNS) and Panama City, FL (PFN). These stations will be specifically referenced later.

Regarding fog formation locally, the observations presented thus far compare favorably with Johnson and Graschel (1992), who analyzed warm air advection cases where surface wind speeds were <8 m s^{-1}, dewpoint depressions were <1.5 °C and air-sea temperature differences were <3 °C which all suggested the potential for dense fog development (NOTE: In their study they used surface visibilities <3.2 km (2 SM) to represent dense fog). The ensuing discussion explores how additional observational (namely MODIS and GOES Products) and short-term model data may be used to assist forecasters when forecasting the development, areal extent and duration of dense fog.

4. Analysis and discussion

a. The decision making process after 0000 UTC 17 February 2011

Various forecast fields from the High-Resolution Rapid Refresh (HRRR) model run by the Global Systems Division of the National Oceanic and Atmospheric Administration's Earth System Research Laboratory are used to assess ingredients and processes supportive of fog formation beyond 0000 UTC 17 February. The HRRR, a 3-km hourly updated inner-nest of the 13km Rapid Refresh, yields outgoing longwave radiation (OLR-W/m^2) escaping from the model's top as a usable operational product. Figure 6 shows the 5-h forecast of OLR flux (valid 0500 UTC 17 February). Around this time, observations began to show developing fog. The maximum OLR is represented by the darkest regions (see annotation in Fig. 6). The cooling is greatest over the area of concern where OLR values of ~250-290 W m^{-2} existed. The HRRR's 5 h forecast of cloud top heights and 6 h forecast of surface visibilities in Figures 7 and 8 (valid 0500 and 0600 UTC, respectively) are also available for further analyses. These sensible weather products can be used along with the previously shown surface and upper air observations to fine tune forecasts of fog formation within the area of greatest OLR. This would be done by determining whether or not the explicit output is consistent with processes that are apt to contribute to locally dense fog formation. These products showed that cloud top heights were forecast to be 1-5 kft (~0.3-1.5 km) while the surface visibilities were forecast <1.6 km (1 SM) over portions of coastal Alabama and the northwestern Florida Panhandle (consistent with the previously shown surface dewpoint depression analysis). The model also continued to forecast light southerly winds (< 8 m s^{-1}) to persist throughout the forecast period (not shown).

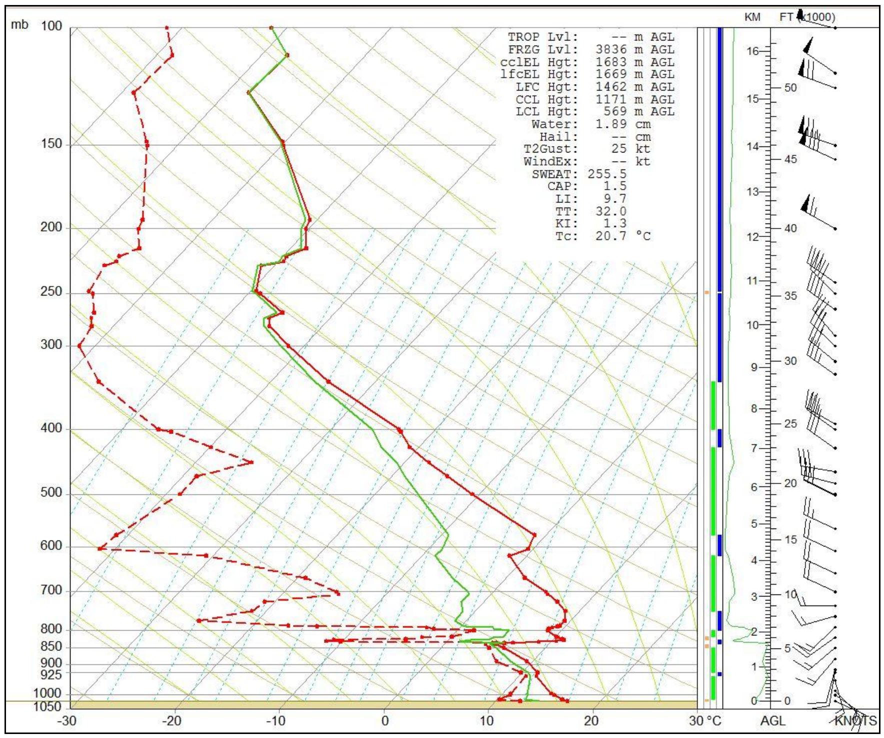

Figure 5. 0000 UTC 17 February 2011 Slidell, LA Sounding (KLIX). Wet bulb temperature profile (°C) is plotted in solid green and wind (kt) profile is given to the right.

In addition to the model output and the MODIS overpasses, the GOES fog product was available to monitor the event throughout the night (Ellrod 1991; Ellrod 1995). Figure 9 is a representative example of the GOES fog product before the first available MODIS overpass at 0410 UTC. Taken at 0145 UTC, the image shows a north-south band of fog/stratus along the Alabama-Mississippi border as well as a few pixels along the Florida panhandle coast and near Mobile Bay. Although not widespread, the GOES imagery is confirming fog development.

b. A mid-point assessment

As the evening progressed, the challenge evolved into the near-term. It is well known that METAR observations are critical when *monitoring* initial fog formation (or non-formation), its horizontal extent and visibilities. However, within the area of concern, METAR observations are rather widely spaced (see Fig. 4) and fog often forms between METAR sites. To assist in this situation, one could use the near temporally continuous GOES spectral difference product, as was done between MODIS overpasses. As with MODIS, the GOES Spectral difference is sensitive to stratus and fog. Although the resolution is better than the METAR station separation (i.e., >50 km average spacing for the area of concern), the GOES product may still miss small pockets of fog due to its coarser resolution. Despite temporal limitations, incorporating the higher resolution (1 km) MODIS data into the forecast process can possibly assist with onset identification and monitoring of dense fog events which ultimately present hazardous impacts to public safety within this U.S. region (e.g., the 1992 Amtrak Train Derailment disaster occurring over the Mobile River Delta and the 1995 Great Mobile Bayway Dense Fog Disaster; Medlin and Croft 1996). Although polar orbiting satellite imagery may not always be directly overhead, it can provide critical high-resolution situational snapshots of evolving event conditions. During this event, the first MODIS pass was available at 0410 UTC (Fig. 10). The MODIS pass is compared with a similarly timed GOES observation in Figure 10.

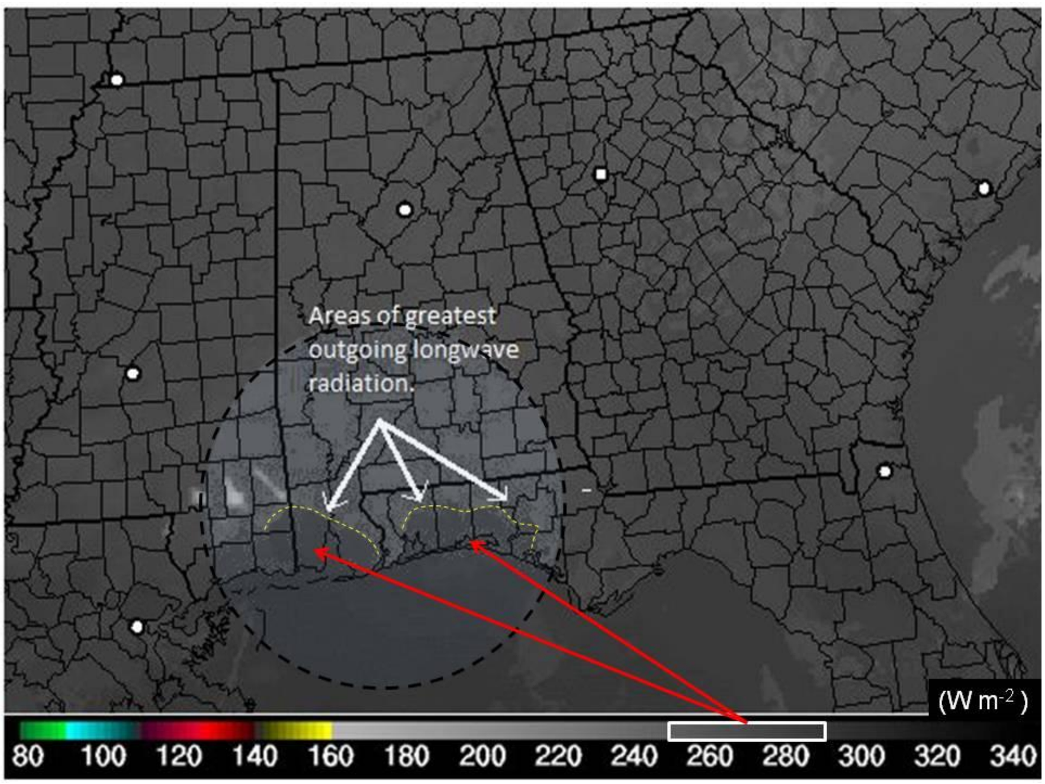

Figure 6. HRRR's 5 h forecast of outgoing longwave radiation flux at the top of the model atmosphere (W m^{-2}) valid 500 UTC 17 February 2011. Data inside of the spyglass was enhanced to show greater contrast between relative values. Coastal areas south of the dashed yellow line represent values from ~250-290 W m^{-2}.

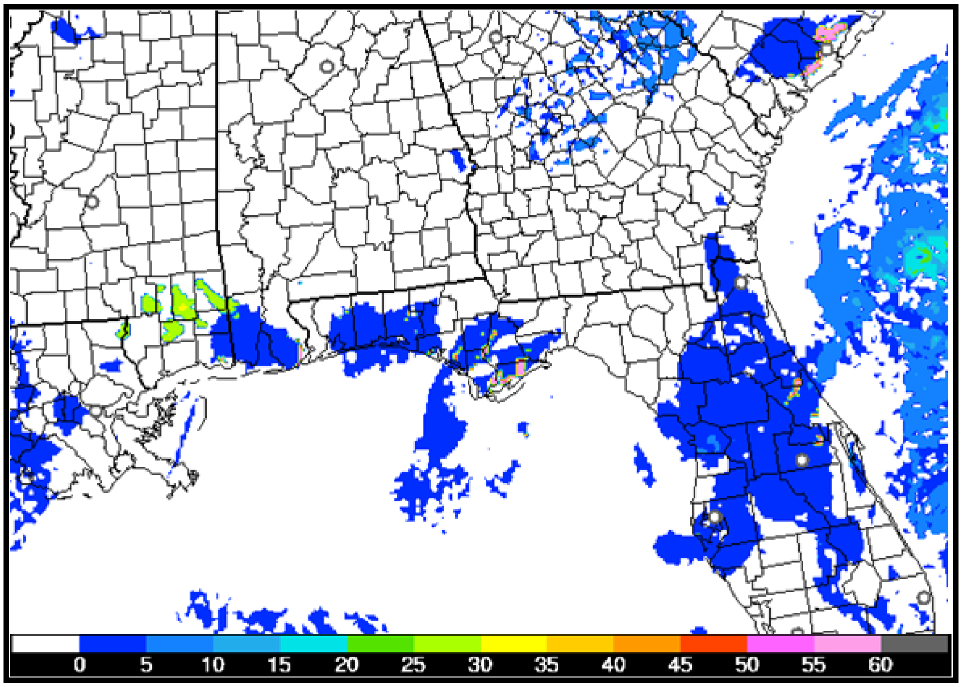

Figure 7. HRRR's 5 h forecast of cloud top heights (kft) valid 500 UTC 17 February 2011. Note that the lowest heights are spatially consistent with the outgoing longwave radiation forecast by the model shown in Fig. 6.

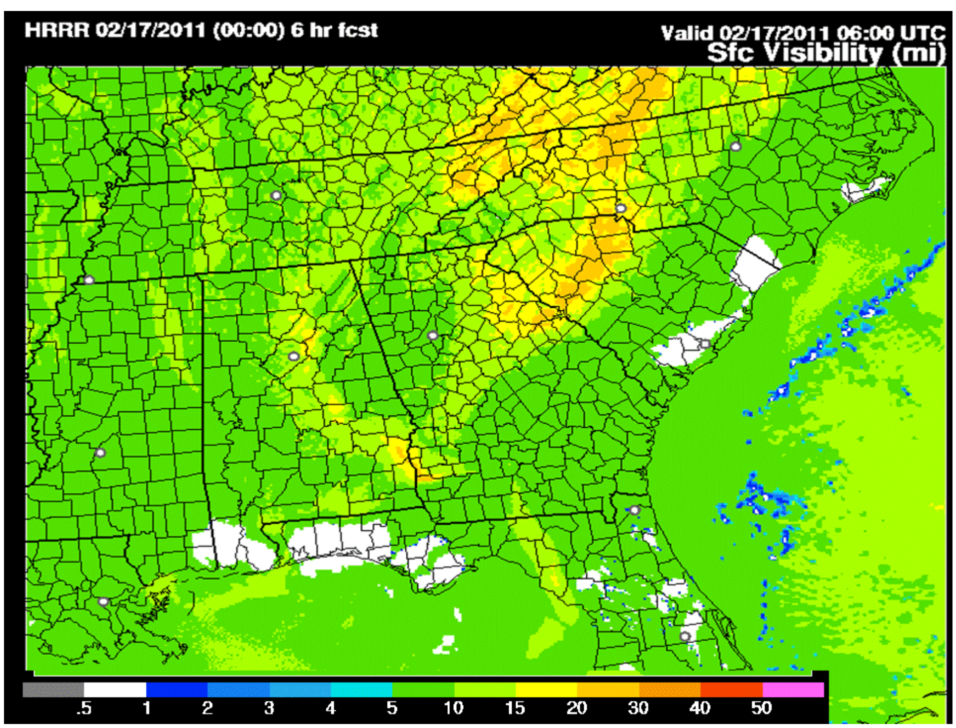

Figure 8. HRRR's 6 h forecast of surface visibility forecast (SM) valid 0600 UTC on 17 February 2011. As with Figure 7, the lowest surface visibilities are spatially consistent with the outgoing longwave radiation forecast by the model shown in Fig. 6.

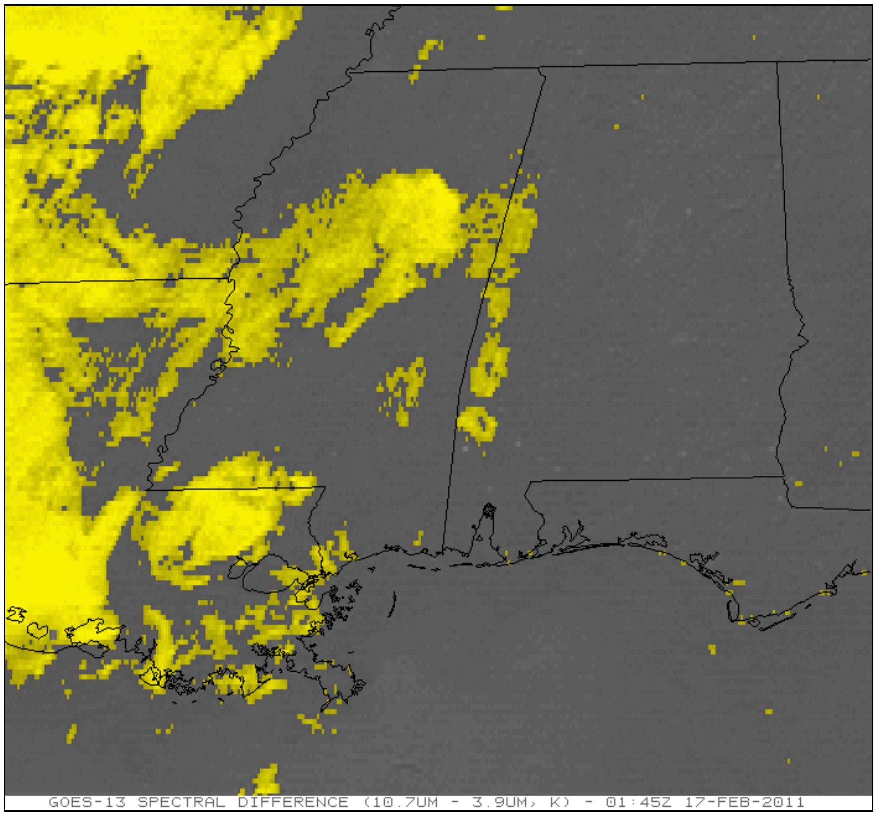

Figure 9. The GOES 4 km “fog product” valid at 0145 UTC on 17 February 2011. The yellow indicates regions of fog and low clouds. This particular observation is respresentative of the GOES observations during the evening leading up to the first MODIS overpass at 0410 UTC (Fig. 10).

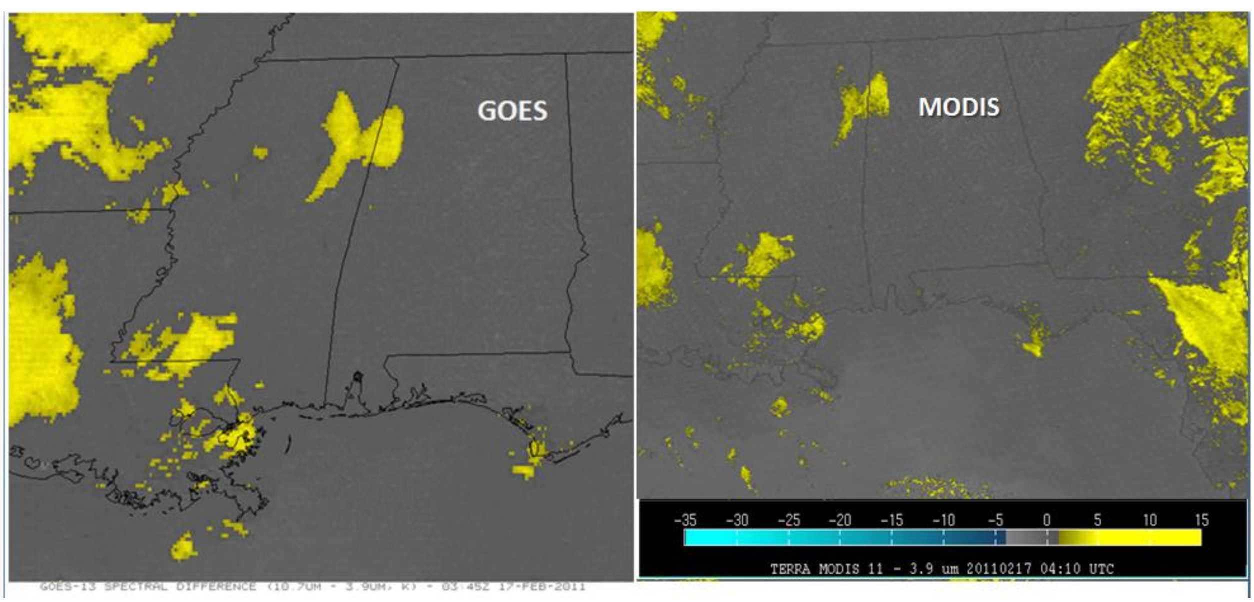

Figure 10. GOES 4 km “fog product” (left – 0345 UTC) and MODIS 1km “fog product”(right – 0410 UTC) both valid on 17 February 2011. The yellow indicates regions of low clouds and fog. Both products observe a similar distribution of fog.

Here, the MODIS spectral difference observed almost no fog along the north Central Gulf Coastal Region. The GOES observations at 0345 UTC also indicate the fog/stratus by Slidell, LA and Panama City, FL although the MODIS imagery is slightly more pronounced inland. GOES did not observe the faint fog signal seen in MODIS at the extreme western Alabama-Florida border, although this may be due to the different times of the observations. At this point, the MODIS overpass lends support to the HRRR's forecast timing of fog onset. Despite this, an operational forecaster would likely continue monitoring the onset and must still consider just how far inland the fog would develop. Figures 11-12 show 4 h model sounding forecasts (initialized 0500 UTC) from the National Centers for Environmental Prediction's Rapid Update Cycle model (RUC 13) for select available coastal and inland sites, respectively (exact locations previously shown in Fig. 4). The 0900 UTC model forecast time was chosen roughly between midnight and sunrise, which is usually a key decision time for NWS forecasters tasked with issuing Dense Fog Advisories. For completeness, a dense fog advisory was issued by 0950 UTC. The figures show that coastal sites indicate saturated conditions in the lowest 200 m while inland sites are approaching saturation below 100 m. Forecast winds were nearly calm below 100 m (not shown) with exceedingly shallow surface based inversions being present at all three of the coastal locations (Fig. 11) whose tops ranged from 30-60 m. A forecaster assessing these data would likely conclude that a fog formation would occur, first near the coast and then inland.

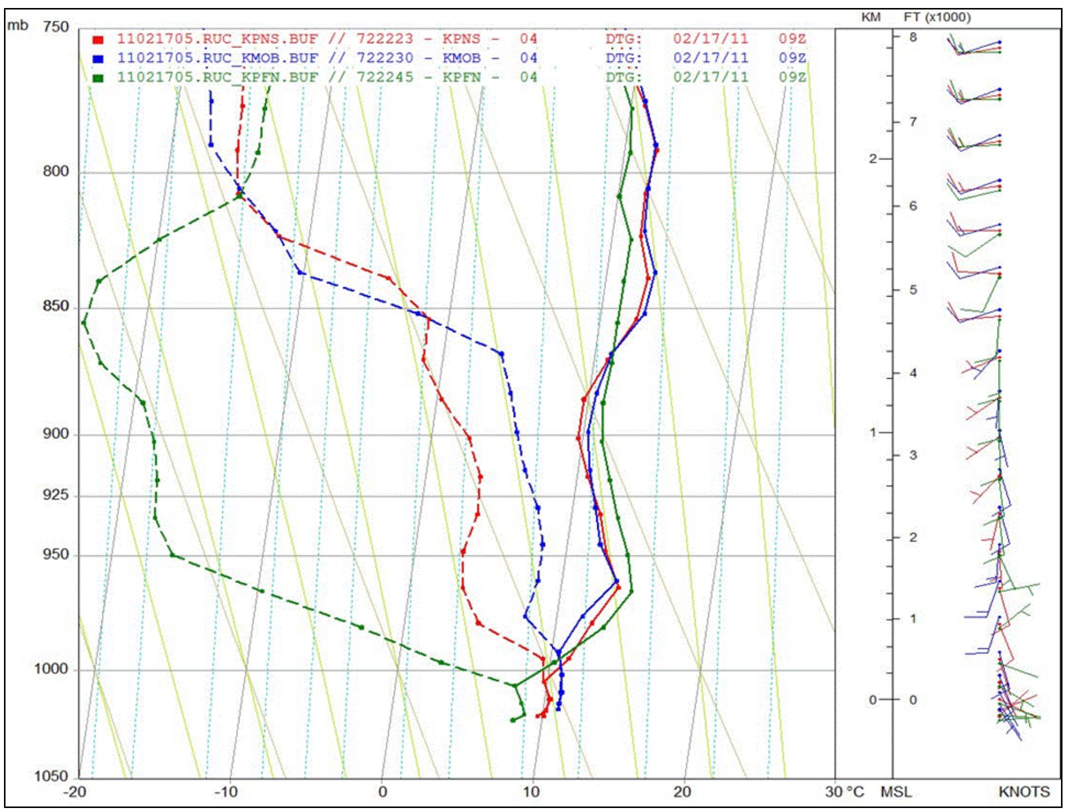

Figure 11. RUC13 4 h BUFR sounding forecast below 750 hPa valid 0900 UTC 17 February for select coastal sites [MOB (blue), PNS (red) and PFN (green)], whose locations are shown in Fig. 4.

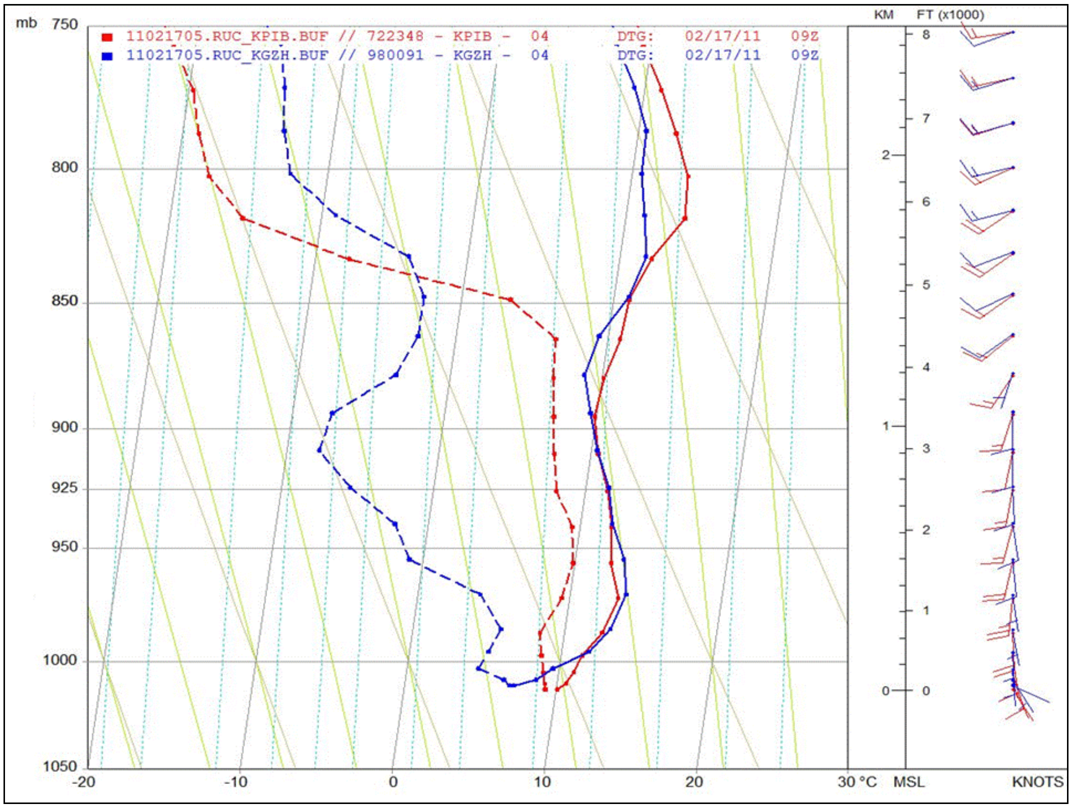

Figure 12. RUC13 4 h BUFR sounding forecast below 750 hPa valid 0900 UTC 17 February 2011 for select inland sites [GZH (blue) and PIB (red), see Fig 4. for locations].

c. Verification of previous forecast thinking with subsequent MODIS passes

There was an ~2.5 h delay before the next MODIS overpass. Meanwhile, the GOES spectral difference product provided continuous observations of fog development. There was little change in the GOES observations until 0545 UTC (Fig. 13). Observations showed further inland penetration of the fog along the Florida panhandle, as seen in MODIS at 0410 UTC, and the development of fog in coastal Alabama. The next MODIS overpass and spectral difference product was available at 0646 UTC and is compared with the corresponding GOES product at 0645 UTC (Fig. 14). Unlike the 0410 UTC MODIS overpass, this one was not positioned favorably. Only the edge covered the eastern boundary of the area of concern, but valuable information was still available. The spectral difference products from both GOES and MODIS compared favorably with the 0643 METAR plots (Fig. 15) and previously demonstrated model forecasts of saturated conditions along the Florida Panhandle. The MODIS spectral difference indicated the region of fog likely developed slightly further inland than the GOES and METAR observations showed. Also, the MODIS observations in the Florida Panhandle indicate a more continuous region of fog. While the 0646 UTC MODIS overpass did not show Mobile Bay, the agreement of the model output to the observations, suggested fog likely had penetrated well inland. METAR observations also showed near calm surface wind conditions, but the earlier onshore wind flow over the cool SSTs and forecasted strong OLR reinforced the idea of fog, potentially dense, developing north of the Interstate 10 corridor.

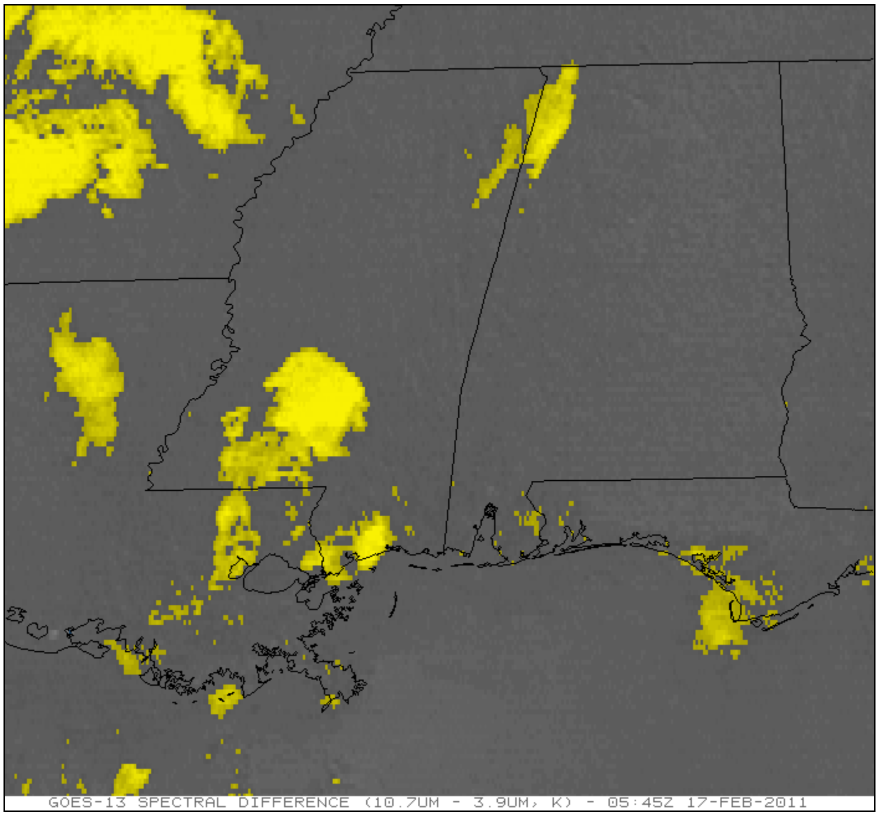

Figure 13. GOES 4 km "fog product" observation valid at 0545 UTC on 17 February 2011.

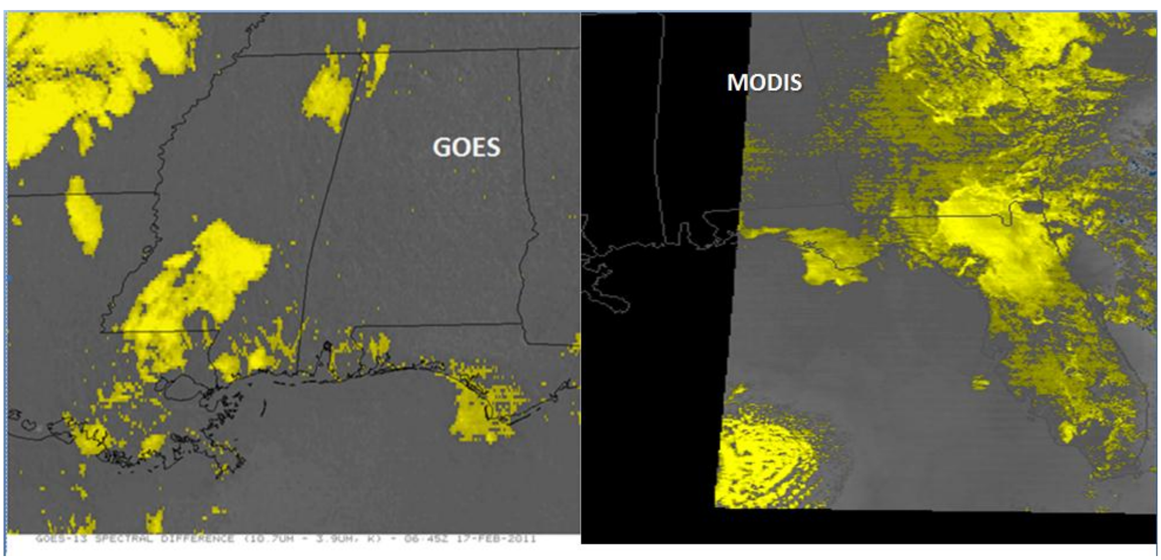

Figure 14. GOES fog product observation (left – 0645 UTC) and MODIS fog product swath (right–0646 UTC) valid on 17 February 2011. The yellow indicates regions of low clouds and fog.

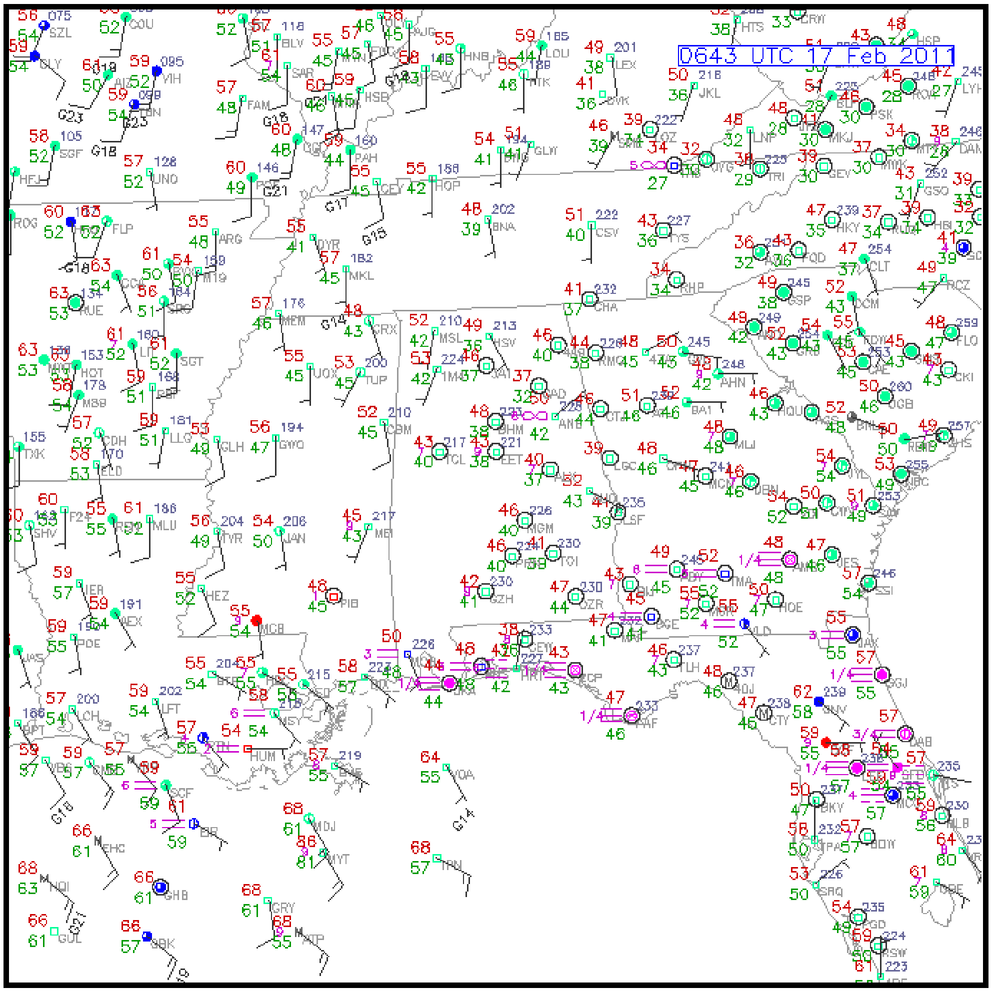

Figure 15. METAR surface observations valid 0643 UTC 17 February 2011. Note how fog is already observed at the coastal stations from Mobile, AL east into the extreme western Florida panhandle. Surface plot is courtesy of NCAR RAP.

The third and final MODIS overpass was valid at 0823 UTC and is compared to the 0845 UTC GOES product (Fig. 16). Again, the pass was not optimal, but it captured most of it. Observed fog and low clouds were now covering much of the area of concern. The importance of the 1 km resolution MODIS fog product was that it not only verified fog development but also confirmed its existence between METAR sites (as did the GOES fog product). It also confirmed the spatial extent of the fog went well beyond what the HRRR forecasted through 0600-0800 UTC. This was critical to the verification of event intensity. The corresponding GOES spectral difference product at 0845 UTC reinforces the observations made by MODIS at 0823. The primary difference is that the MODIS product observations show a more contiguous fog/stratus field versus GOES. MODIS shows patches of fog/stratus extending further north than GOES, primarily due to the 1 km resolution (also refer back to Figure 1).

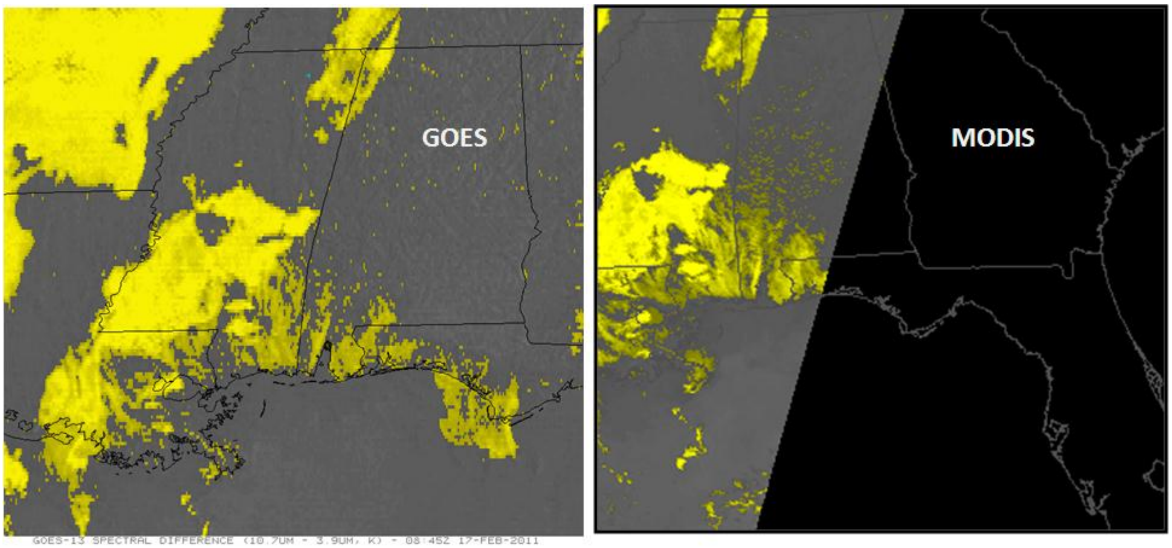

Figure 16. MODIS fog product swath valid 0823 UTC 17 February 2011. The yellow regions indicate low stratus or fog. The indication is dense fog is surrounding Mobile Bay, like the HRRR output, but also shows fog and low clouds extending well inland.

5. Conclusions

Local fog formation ultimately depends on microscale and mesoscale processes acting within the boundary layer. This makes the successful forecast of fog formation, extent, duration and intensity even more uncertain. While during the event of 17 February 2011 forecasters may have concluded that dense fog formation was more likely along the coast given an acute knowledge of the local climatology, prevailing synoptic conditions, supportive ingredients and processes, they would have been less certain of its maximum inland extent, duration and intensity. Despite an arsenal of modern day forecast tools which were all highly suggestive of fog formation along the coastal zone, the event also showed dense fog developed much further inland than what was forecast by the model (both implicitly from an analysis of the processes and ingredients and explicitly by sensible direct model output). This observation lends itself to the notion that predicting the onset location and time is just one challenge, but continual monitoring is needed to follow through if the maximum extent of a successful forecast is to be realized. In short, a forecaster, using all available observational data, must know how to adjust their thinking ‘on the fly.’

As the event unfolded, forecasters would have been able to nudge the forecast in the right direction at key decision points in time. For example, the MODIS fog product indicated fog had developed well before the first visible GOES imagery just after sunrise. Additionally, the earlier MODIS passes (0410 and 0646 UTC) provided observational confirmation of the timing and location of fog forecast by the HRRR. And finally, although the 0646 UTC MODIS overpass did not show Mobile Bay, the agreement of the model output to the observations, suggested fog likely had penetrated well inland and this was verified by surface observations. Despite its coarser resolution, the GOES data will remain invaluable towards filling in gaps between MODIS passes thereby remaining a staple in this type of forecast situation. All of this gives forecasters more information to pass along to early morning commuters to assist with decisions regarding an ongoing dense fog advisory or may have prompted issuance if none were previously in effect.

By reconstructing a forecaster's potential thought processes for this event, this paper has demonstrated how MODIS satellite imagery may be used in concert with high resolution short term mesoscale model forecast fields, and existing GOES observations, to help ascertain event setup and maintain situational awareness. Looking to the future, this case highlights one of the exciting prospects of GOES-R, which will be able to provide a spectral difference product at a resolution similar to MODIS, but with the advantage of being in a geostationary orbit.

Acknowledgements. The authors wish to thank Mr. Frank LaFontaine (NASA SPoRT) for recreating the MODIS SST and spectral differences images for this event, Mr. Kevin McGrath (NASA SPoRT) for processing the archived GOES spectral difference products, and Dr. Paul Croft (Kean University) for providing a helpful review of this paper. Finally, we also wish to thank the reviewers for their time in providing invaluable suggestions and comments to solidify this paper.

REFERENCES

Barnes, W. L., T. S. Pagano, and V. V. Salomonson, 1998: Prelaunch characteristics of the Moderate Resolution Imaging Spectroradiometer (MODIS) on EOS-AM-1. *IEEE Trans. Geosci. Remote Sensing*, **vol. 36**, pp. 1088-1100.

Croft, P.J., R. L. Pfost, J. M. Medlin, G. A. Johnson, 1997: Fog Forecasting for the Southern Region: A Conceptual Model Approach. *Wea. Forecasting*, **12**, 545-556.

____, D. Darbe, and J. Garmon, 1995: Forecasting significant fog in southern Alabama. *Natl. Wea. Dig.*, **19,** 10–16.

Ellrod, G.P., 1995: Advances in the Detection and Analysis of Fog at Night Using GOES Multispectral Infrared Imagery. *Wea. Forecasting*, **10**, 606-619.

___, 1991: Nighttime fog detection with bi-spectral GOES-VAS imagery. *Proc. Fourth Int. Conf. on Aviation Weather Systems*. Paris, France, Amer. Meteor. Soc., 71-75.

Eyre, J.R., J.L. Brownscombe and R. J. Allan, 1984: Detection of fog at night using Advanced High Resolution Radiometer (AVHRR) imagery. *Meteor. Mag.*, **113**, 66-271.

Guenther, B., G. D. Godden, X. Xiong, E. J. Knight, S. Qiu, H. Montgomery, M. M. Hopkins, M. G. Khayat, and Z. Hao, 1998: Prelaunch algorithm and data format for the Level 1 calibration products for the EOS-AM1 Moderate Resolution Imaging Spectroradiometer (MODIS). *IEEE Trans. Geosci. Remote Sensing*, **vol. 36**, pp. 1142-1151.

Hastings, D.A., and W.J. Emery, 1992: The advanced very high resolution radiometer (AVHRR) – A brief reference guide. *Photogramm. Eng. Remote Sens.*, **58**(8), 1183-1188.

Jedlovec, G., F. LaFontaine, J. Shafer, J. Vazquez, E. Armstrong, and M. Chin, 2009: An enhanced MODIS / AMSR-E SST composite product. *Symposium Proceedings GHRSST User Symposium*, Santa Rosa, CA, 3 pp.

Johnson G. A. and J. Graschel, 1992: Sea fog and stratus: A major aviation and marine hazard in the northern Gulf of Mexico. Preprints, *Symp. on Weather Forecasting*, Atlanta, GA, Amer. Meteor. Soc., 55–60.

Maturi, E., A. Harris, and J. Sapper, 2010: A new ultra high resolution sea surface temperature analysis from GOES-R and NPOESS-VIIRS. *6th Symposium on Future National Operational Environmental Satellite Systems-NPOESS and GOES-R*, Amer. Meteor. Soc., Atlanta, GA, P321.

Medlin, J.M. and P.J. Croft, 1996: An Examination of the Mobile Bayway Fog Disaster. Preprints, *15th Conference on Weather Analysis and Forecasting*, Norfolk, VA, Amer. Meteor. Soc.,

STAR: www.star.nesdis.noaa.gov/sod/mecb/blended_validation/index.php

Wentz, F., and T. Meissner, 2004: AMSR-E/Aqua L2B Global Swath Ocean Products Derived 358 from Wentz Algorithm V002, various dates, http://www.nsidc.org/data/amsre, National Snow 359 and Ice Data Center, Boulder, Colorado, USA.